SMU Journal of Undergraduate Research

Volume 8 | Issue 1 Article 2

January 2024

Radon Plate-out and the Effects of Airflow and Electric Charge for Dark Matter Experiments

Faith Fang
Southern Methodist University, faithf@smu.edu

Radon Plate-out and the Effects of Airflow and Electric Charge for Dark Matter Experiments

Cover Page Footnote

I would first like to thank Dr. Jodi Cooley and Taylor Wallace for their guidance and mentorship throughout this research project, and for building a strong foundation for future work in radon plate-out. In addition, I would also like to thank Dr. Robert Calkins for his advice, patience, and support. Through numerous coding issues and revisions, his advice has been invaluable in the development of this work. Dr. Calkins also showed me what it truly looks like to pursue curiosity and learning as the foundation of scientific research. This thesis would not have been possible without his contributions. Lastly, I want to thank my parents and brother for their encouragement throughout the highs and lows of my undergraduate career, and for walking alongside me to the finish line. This material is based upon work supported by the National Science Foundation under Grant No. 2111457, the Hamilton Scholars Program, the Grand Challenge Scholars Program, and the SMU Physics Department. Any opinions, findings, and conclusions or recommendations expressed in this material are those of the author(s) and do not necessarily reflect the views of the National Science Foundation.

Radon Progeny Plate-Out and the Effects of Airflow and Electric Charge for Dark Matter Experiments

Faith Fang[1]

faithf@smu.edu

Robert Calkins[1]

ABSTRACT

The Cryogenic Dark Matter Search (SuperCDMS) is an international collaboration designed to search for and detect dark matter particles, which make up ~85% of the matter in the universe. The plate-out, or deposition of naturally occurring radioactive decay byproducts onto surfaces, can create backgrounds that interfere with dark matter detection experiments. In the first series of these experiments, we analyze the amount of radon progeny, ^{214}Pb and ^{214}Bi, that plate-out on polycarbonate samples while controlling factors such as electric charge and airflow. These samples are exposed to radon-spiked nitrogen gas in a polycarbonate wind tunnel to simulate plate-out conditions in a controlled environment. To determine radon progeny plate-out rates for each trial, the initial activity of radon progeny is calculated from the measurements of an Ortec alpha counter. In previous iterations of the experiment, we observed static charge buildup on surfaces, especially polycarbonate. This charge buildup was reduced by the implementation of an electric field source in the wind tunnel, yielding more consistent polycarbonate trials. After neutralizing the electric charge on polycarbonate, the second series of the experiment compares normalized radon daughter plate-out for polycarbonate and copper samples. Copper measurements demonstrated a positive correlation between air speed and radon daughter plate-out rate from speeds of 0 to 60 ft/min, stabilizing at speeds between 0 to 60 ft/min. Acrylic measurements demonstrated no observable relation between air speed and normalized plate-out rates. Results from both results deviate from the linear correlation of air speed and plate-out rate predicted by the Jacobi plate-out model [1]

1. INTRODUCTION

The Super Cryogenic Dark Matter Search (SuperCDMS) is an international collaboration of institutions seeking to detect dark matter particles down to ten times lighter than the mass of a proton, though the range can include masses up to 100 times heavier. With observations indicating that ~85% of the matter in the universe is made up of dark matter, the detection of these particles is crucial for future developments in physics [2]. The SuperCDMS experimental facility is based in an underground laboratory in Canada known as SNOLAB. This is to shield the detector from high energy cosmic ray particles and from radioactive decay byproducts [4]. These radioactive decay byproducts include radon, a naturally occurring element with the potential to cause long-term contamination, given an exceptionally long half-life. Radon is of high interest given that its decay products can mimic the dark matter particle signature and produce background events. For dark matter experiments, contamination from radon can be reduced through the study of the interactions of radon decay products with common materials involved in the experiments.

In this experiment, we explore radon progeny plate-out on polycarbonate and copper. These two materials were selected given their relevance to the dark matter detectors and detector storage. The detectors are stored in acrylic purge cabinets during construction, and each detector is housed in copper, as shown in Figure 1. Thus, our experiment seeks conditions that reduce radon progeny plate-out for polycarbonate and copper, so that the storage and transportation of detectors can be improved. This supports the future sensitivity and precision of the detectors by eliminating background noise.

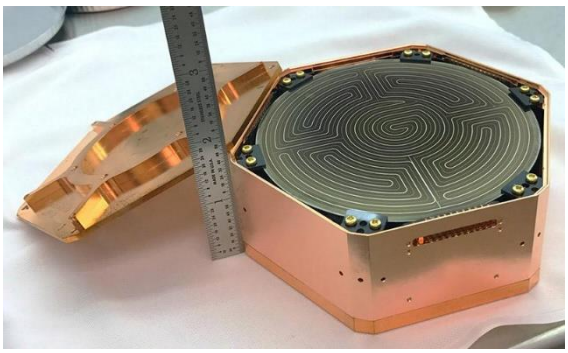

Figure 1: SuperCDMS Dark Matter Detector [2]

The research from this experiment uses experimental runs with a wind tunnel and a Pylon radon source to simulate real-world conditions of airflow and determine the conditions for minimizing radon progeny plate-out. The air speed (0, 60, 133, or 150 ft/min) and sample material (copper or polycarbonate) are varied to observe trends and determine the conditions that minimize plate-out. Since the material traits differ between copper and polycarbonate, factors of charge buildup are addressed with

[1] Department of Physics, Southern Methodist University

a number of processes, most effectively by generating an alternating electric field to attract charged decay particles. Lastly, the data is analyzed, revealing differences in radon progeny plate-out trends for polycarbonate and copper.

A. *Radon Decay Chain*

A ^{222}Rn progeny, ^{210}Pb, has a 22.3-year half-life that could cause long-term contamination for the SuperCDMS experiment. It is therefore critical to understand the behavior of radon progeny plate-out on different materials used in the experiment. Radon naturally occurs from the decay of ^{238}U, which exists in high amounts underground in rocks. Gaseous radon decays through alpha decays and other progeny that can plate-out, or stick, onto detectors. The alpha decays from ^{222}Rn and its progeny reduces detector sensitivity to detect dark matter.

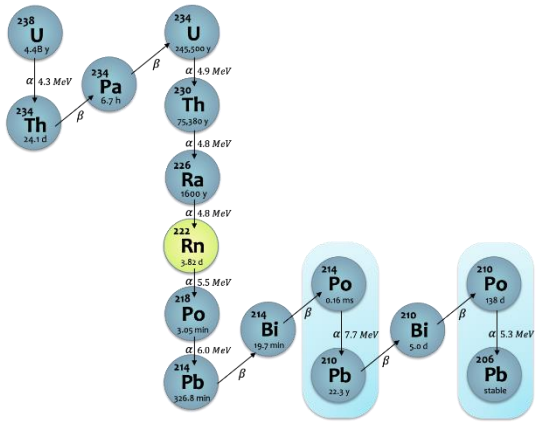

Figure 2: Uranium-238 decay chain

As shown in Figure 2, the decay chain of ^{238}U involves the emission of energy through ionizing radiation, which includes alpha and beta particles [3]. The following segments of the decay chain describe the radionuclides, or unstable atoms that are formed in radioactive decay. For this experiment, the Pylon RN-1025 contains dry radium (^{226}Ra) that provides calibrated quantities of radon (^{222}Rn) when nitrogen gas flows through the source. The ^{222}Rn decay chain includes two key alpha decays from ^{214}Po to ^{210}Pb and ^{210}Po to ^{206}Pb, which emit energies of 7.7 MeV and 5.3 MeV respectively. The nuclide ^{210}Pb has a half life of 22.3 years, and during its alpha decay, the recoiling nucleus produces an ionization signal similar to that of dark matter, thus creating background for the SuperCDMS experiment [5].

The normalized counts of initial ^{214}Pb and ^{214}Bi (normalized to airborne radon concentration) described above are measured over repeated experimental runs to offer a comparison of the radon progeny plate-out given a variety of factors. These factors include electrical charge, air speed, sample material, exposure time, and rate of radon-spiked nitrogen gas.

B. *Equations of Decay*

Radioactive decay involves a radioactive atom giving off radiation in the form of energy or particles to reach a more stable state. This process of decay occurs randomly, with a rate described by the half-life, which is generally unique to each nucleus type. The half-life quantifies the length of time for half of the radioactive atoms of a radionuclide to decay on average. This is at a statistically constant rate; therefore, by measuring the activity of Bi and Pb on a sample over time, we can extrapolate back to the number of initial parent Po atoms [6].

The law of radioactive decay provides a mathematical decay probability per unit time, expressed as:

$$\lambda = \frac{-dN/dt}{N} \qquad \text{(Eq. 1)}$$

where N is the number of radioactive nuclei, -dN/dt is the decrease of this number per unit of time, and λ is the decay constant, or the probability of decay per nucleus per unit of time. This is specific for each nuclide decay mode. The decay rate or activity A is then defined as the number of decays per unit of time, as seen in Eq. 2.

$$A = -\frac{dN}{dt} = \lambda N \qquad \text{(Eq. 2)}$$

This decay rate is then integrated and evaluated at boundary conditions of t=0 and $N=N^0$, the initial number of atoms, to find

$$\ln\left(\frac{A}{A^0}\right) = -\lambda t \qquad \text{(Eq. 3)}$$

The activity as a function of time depends on just the decay constant and initial number of parent atoms, and can be expressed as:

$$\mathrm{A} = \mathrm{A}^0 e^{-\lambda t} \qquad \text{(Eq. 4)}$$

To determine the amount of daughter nuclei in a branching decay with two decays, the above equations can be used to solve the following differential equation, which considers radioactive decay and radioactive in-growth by decay of the parent nuclei λ_1:

$$\frac{dN_2}{dt} = -\lambda_2 N_2 + \lambda_1 N_1 \qquad \text{(Eq. 5)}$$

The solution yields the equation:

$$A_2 = \lambda_2 N_2 = \frac{\lambda_2}{\lambda_2 - \lambda_1} A_1^0 (e^{-\lambda_1 t} - e^{-\lambda_2 t}) \qquad \text{(Eq. 6)}$$

which can be applied to our experiment to calculate the amount of daughter nuclei from ^{214}Po as a function of ^{214}Bi and ^{214}Pb activities. This equation assumes no initial atoms from the daughter nuclei, with all amounts resulting from the radioactive decay.

For our experiment, the measurements of ^{214}Po activity over time are used to calculate the activity of two nuclides, ^{214}Bi and ^{214}Pb. ^{214}Pb has a half-life of 326.8 minutes, decaying to ^{214}Bi, a daughter nuclide with a half-life of 19.7 minutes. Then, ^{214}Bi decays into its daughter nuclide, ^{214}Po. With the ^{214}Pb half-life exceeding the half-life of ^{214}Bi, the ^{214}Bi activity will disappear at a higher rate, leaving only the ^{214}Pb activity to decay. The two activities are summarized as a total activity. As shown later in the paper, this activity behaves as a rapid decline when both the

^{214}Bi and ^{214}Pb activities are decaying, followed by a slower decay of ^{214}Pb activity.

C. *Jacobi Model*

The Jacobi model offers an estimation of radon progeny plate-out rate by simplifying the plate-out process as an average over all atoms in the room [1]. This model can be summarized with Equation 7, where a room of volume V, surface area, S, deposition velocity, v, and air circulation rate, R, has a deposition rate of λ_D = vS/V and a radon progeny filtration rate of λ_F = R/V. The ^{218}Po decay rate, λ_1, is 13.37 hr^{-1}, and λ_0 refers to the decay constant for radon. The concentration of plate-out daughter atoms per unit area on the sample, C_S, is proportional to the concentration of radon atoms in the air, C_{air}, which is measured in units of (Bq/m^3).

$$\lambda_1 C_S = \lambda_0 C_{air} \times \frac{v}{\lambda_D + \lambda_F + \lambda_1} \qquad \text{(Eq. 7)}$$

In applying the Jacobi model to the wind tunnel, the filtration rate λ_F would be zero, as there is not a radon mitigation system in place [7] [8]. Therefore, the equation simplifies to:

$$\lambda_1 C_S = \lambda_0 C_{air} \times \frac{v}{vS/V + \lambda_1}$$

To determine the plate-out response at low velocities and high velocities, we take the limit as v approaches zero and infinity. This is when the deposition rate term is significantly less than or greater than the ^{218}Po decay rate.

$$\lim_{v \to 0} = \lambda_0 C_{air} \frac{v}{\lambda_1} \qquad [\frac{vS}{V} \ll \lambda_1]$$

$$\lim_{v \to \infty} = \lambda_0 C_{air} \frac{v}{vS/V} = \lambda_0 C_{air} \frac{V}{S} \qquad [\frac{vS}{V} \gg \lambda_1]$$

At low velocities, the model displays a linear response, where the plate-out rate would increase as a function of air speed. However, as seen for higher velocities, the deposition term dominates, which leads towards a constant plate-out rate.

The Jacobi model offers an approximation of the relationship between radon concentration in the air C_{air} and the deposition of radon progeny on a surface. Based on the velocity term, one would expect a linear relation between velocity and plate-out rate, where greater deposition velocity leads to a higher deposition rate on the surface of a sample for low velocities.

2. EXPERIMENTAL PROCEDURE

The experimental setup is displayed below in Figure 3. An N2 dewar supplies nitrogen gas to the experiment. The N2 gas flow rate is maintained at 4 standard cubic feet per hour (SCFH) using a flow meter. This flows through the Pylon RN-1025 source to pick up gaseous ^{222}Rn. This is then supplied to the wind tunnel, which includes a computer fan operating on a voltage input to create a certain airspeed within the tunnel. The field source, which is connected to the voltage input, helps to minimize the charge buildup inside the wind tunnel by attracting free electrons to one side of the tunnel. As the spiked N2 gas circulates through the wind tunnel during an exposure, it is allowed to exit through an exhaust hood. Gas from the wind tunnel also passes through the Rad7, which records the equilibrium radon levels, relative humidity, and temperature of the gas in the wind tunnel. Each exposure ranges from 12-24 hours, as this gives the gas in the wind tunnel ample time to reach a steady-state level of radon.

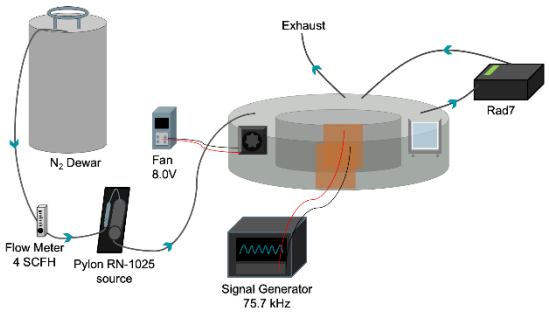

Figure 3: Wind Tunnel and Experimental Setup of N2 Airflow

To remove radon progeny from the samples and prepare them for exposure, a cleaning procedure is used [9]. Each sample is hand-cleaned in a three-step process. First, the sample is sprayed with Radiacwash and allowed to rest for ~1 minute to remove the radioactive elements present on the sample. After being wiped, distilled water is used to rinse and wipe the Radiacwash spray off. Then, isopropyl alcohol is applied to wipe down and dry the sample. Since isopropyl alcohol removes permanent marker labels on a sample, the five points and sample name are redrawn on the sample.

To check for significant initial activity, the sample is placed in the Ortec Alpha Counter, and a 10-15 minute background measurement is taken. Once the background measurements are taken, and there are no counts measured within the expected channels for radon progeny plate-out, the sample is removed from the Ortec and allowed to rest with the antistatic fan turned on for ~1 minute to remove charge buildup. The sample is then placed into the wind tunnel for a 12-24 hour exposure. After the exposure, the sample is quickly removed and moved to the Ortec to begin the measurement of alpha decays. This transfer time from the end of the exposure to the start of Ortec measurement is recorded as a time delay factor when calculating the initial activity of plate-out. The Ortec is then allowed to run for 12-24 hours, while another sample is placed in the wind tunnel for the next exposure. Trials are staggered so that exposures and Ortec measurements can be conducted simultaneously.

A. *Pylon RN-1025 Source*

The conditions of environmental radon gas are simulated by a Pylon RN-1025 source, shown in Figure 4. This source contains powdered radium, ^{226}Ra with an activity of 34 kBq, which decays into gaseous ^{222}Rn. This gaseous ^{222}Rn disperses into the wind tunnel when nitrogen, or N2 gas, is supplied through the source. For this experiment, the flow of radon-spiked N2 gas is maintained

at 4 SCFH throughout the exposure, with an exhaust line removing excess gas from the wind tunnel.

Figure 4: Pylon RN-1025 Source [16]

B. *Polycarbonate vs. Copper*

While this experiment examines the radon progeny plate-out on both polycarbonate and copper samples, it is important to acknowledge fundamental differences between the two materials. Copper is present in the housing and cryostat of the dark matter detectors, as seen in Figure 5. As a material used in close proximity to the experiment, the effects of plate-out are of particular interest. However, copper is a conductor, so charges can freely move to reduce the electric field or leave the sample. Former experiments tested the effects of airflow on copper and determined an increase in radon progeny plate-out when airflow is present [10]. Therefore, this experiment aims to recreate and compare copper studies with the data collected from polycarbonate samples.

Plastics are present in purge cabinets and storage devices for the SuperCDMS experiment, and they are therefore important materials to study. However, plastic presents problems as an insulator; electric charge can build up on the sample, and charge measurements on plastics are notoriously inconsistent [11]. Electric charge could affect plate-out results, as alpha particles have a +2 electrostatic charge and may be attracted or repelled by charges in the polycarbonate. This is observed in the thesis by Bruenner, which demonstrates such results [11]. To obtain comparable results for radon progeny plate-out, the possible confounding variable of charge build-up was addressed with a number of tools.

C. *Electric Charge on Polycarbonate*

In early polycarbonate runs, electric charge build up was observed to increase after the background Ortec run and wind tunnel exposures. Electric potential was measured with an electrostatic meter at five points on each polycarbonate sample, as pictured in Figure 5. The measurements of electric potential could vary by over 1500 V across the five points, further highlighting the necessity of normalizing or reducing electric charge on the sample. This can be seen in the results of Figures 6 and 7.

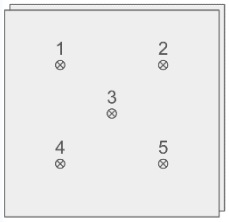

Figure 5: Polycarbonate electric potential measurement locations

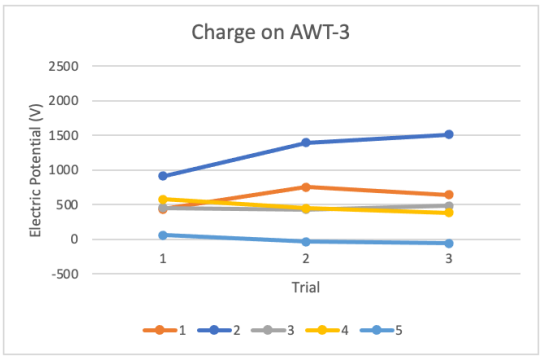

Figure 6: Electric potential measurement on AWT-3 acrylic sample, control run over 24 hours

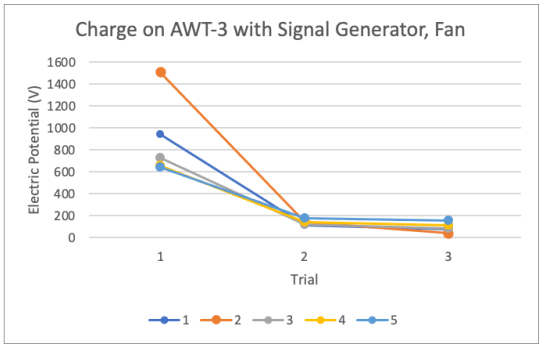

Figure 7: Electric potential measurement on AWT-3 acrylic sample using field source and antistatic fan over 24 hours

D. *Charge Mitigation Equipment*

Early attempts to address the electric charge buildup on acrylic samples involved using an antistatic fan [12] and a Zerostat 3 [13] between the Ortec background run and the wind tunnel exposure. This equipment is pictured below in Figure 8. The trigger on the Zerostat 3 is pressed to neutralize static charge on part of the sample, and the antistatic fan was used to blow air over the sample while resting to eliminate any additional charge.

Figure 8: Antistatic fan and Milty Zerostat 3 antistatic gun

While these two instruments aided in reducing initial charge before the exposure, another issue of charge buildup arose during exposures. As air was blown throughout the wind tunnel, charges accumulated on the sample during the exposure itself, thus leading to charge buildup on the sample in what we suspect is due to the triboelectric effect. This can be seen in Figure 6, where the electric potential on the acrylic sample began with a range of nearly 1000V, but increased to a range of over 1500V following the exposure.

Therefore, we constructed a field source that created an alternating electric potential to reduce charge buildup during the exposure. This field source was created by two copper foil sheets affixed to the two sides of the internal walls in the wind tunnel, with a signal generator connected and generating an alternating potential. One sheet was connected to the positive signal, while the other was connected to a negative signal. When the signal generator was turned on, an alternating potential with a frequency of 75.7 kHz was supplied to either side of the copper foil, creating an electric field that would attract charged particles to one side of the tunnel as they flowed with the air. This was intended to reduce charge in the air that could stick to the sample and cause charge buildup [9]. This setup is displayed below in Figures 9 and 10.

Figure 9: Signal Generator for field source

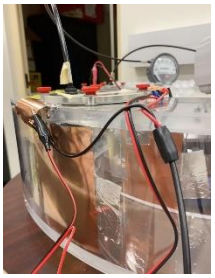

Figure 10: Field source alternating signal copper foil setup

As seen in Figure 11, the results of using both a field source and the antistatic fan were quite effective in charge neutralization on a sample by the end of the trial runs. After conducting 14 experimental runs of acrylic samples using the field source, the results for the ^{214}Pb and ^{214}Bi normalized plate-out were plotted as a function of the percent reduction of electric charge. This charge reduction efficiency percentage is estimated as the reduction of potential from measurement at the start of the run and the end, divided by the initial potential. This is shown below in Figure 11, with the data displayed in the appendix. As noted by the cluster at 100% charge reduction, the field source and antistatic fan produced replicable plate-out rates within a range of 0.05 m^3/s given similar electric charge reduction percentages. This is with the exception of the outlier at 140% reduction, which is excluded as a data point because it deviates more than 3 standard deviations from the distribution. While the reason for this outlier is unknown, it also demonstrates how prone acrylic is to electric charge inconsistencies [14]. Given the success of the new field source, we proceeded to use the charge mitigation setup in the next step of the experiment: measuring the plate-out of copper and acrylic samples.

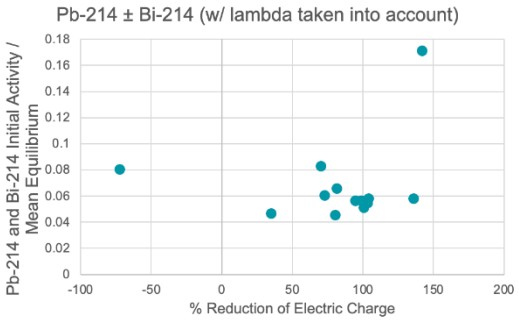

Figure 11: ^{214}Pb and ^{214}Bi normalized plate-out rate vs % reduction of electric charge

3. ANALYSIS

A. *Calculating Initial Activity*

The Ortec detects the alpha spectrum with counts of decays, using channel numbers that are calibrated to be linearly proportional to energy. The counts, separated by channel numbers, are calibrated using the energy of ^{210}Pb, which emits an alpha with an energy of 5.3 MeV. The energy is proportional to the channel number by the following relation:

$$E = k(Channel) \qquad \text{(Eq. 8)}$$

where k is the calibration constant that is used to calculate the energy at each channel. Then, knowing the expected energy emitted by ^{214}Po, these values are used to isolate the number of counts of ^{214}Po in our runs and use the energy emitted over time to extrapolate the number of ^{214}Bi and ^{214}Pb atoms that plated out on the sample initially. These measurements allow us to monitor the decay of the isotope over time, which is used to determine the activity for each isotope within the energy window. A fit function written in Python, which is referenced in Eq. 7, calculates the counts and initial activity of ^{214}Pb and ^{214}Bi. The number of decay counts is measured in 30-second, 10-minute, and 30-minute data files. For this analysis, the measurement of the ^{214}Po peak is used to extrapolate the amount of ^{214}Pb and ^{214}Bi, given the known decay rates and decay over time. An example of these plots is shown below in Figures 12 and 13.

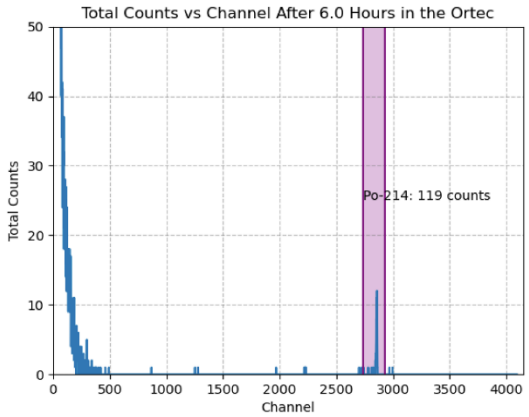

Figure 12: Po-214 counts for WT-1 copper sample at 6V

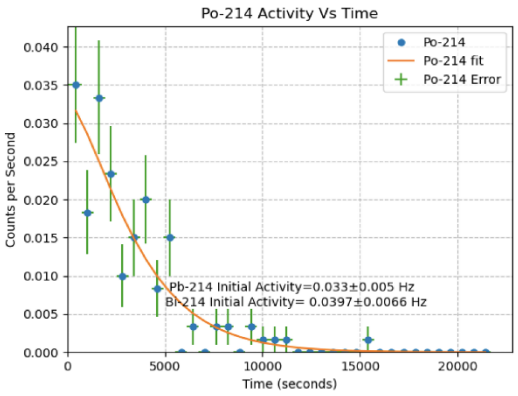

Figure 13: ^{214}Pb and ^{214}Bi initial activity vs. time for WT-1 copper sample at 6V

Initial activity of ^{214}Pb and ^{214}Bi are found from Eq. 6. Activity is related to the number of atoms as a function of decay rate, as seen in Eq. 9. Therefore, the number of atoms can be calculated by multiplying

$$A = \lambda N = \frac{N}{\tau} = \frac{N}{t_{1/2}/\ln(2)} \qquad \text{(Eq. 9)}$$

$$N = \frac{A}{\lambda} \qquad \text{(Eq. 10)}$$

The number of atoms N of ^{214}Pb and ^{214}Bi are separately analyzed and compiled to determine trends on acrylic and copper. These atom counts can then be combined to find the total number of plate-out atoms on each sample. The equilibrium concentration of radon in the air during the wind tunnel exposure, measured by using the Durridge Rad7, can then be used to calculate the radon concentration of the atmosphere of the wind tunnel, which is defined as the number of becquerels per unit volume (Bq/m^3). This relation, defined as the normalized radon progeny plate-out rate, is found by dividing the number of atoms by the average radon level equilibrium.

Using this procedure, 29 acrylic trials and 14 copper trials conducted at fan voltages of 0, 6, 8, and 10 V were analyzed and plotted for each material. Table 1 offers the air speed conversion from the anemometer, an instrument for measuring wind speed. The fan voltages correspond to the following air speed measurements from the anemometer. These values were based on previous experimental data using the same experimental setup [15].

Fan Voltage (V)	Air Speed (ft/min)
0	0
6	60
8	133
10	150

Table 1: Fan Voltage to Air Speed Conversion

4. RESULTS AND DISCUSSION

Figures 14 - 19 show the radon progeny plate-out rates of ^{214}Pb and ^{214}Bi in relation to air speed for acrylic and copper samples. The 2-parameter polynomial fit is performed on the data, as shown by the red line. The blue line is the low-velocity Jacobi model prediction, which offers a one-parameter linear model. Many of the figures below demonstrate that the Jacobi model does not adequately describe the data, even with the larger uncertainties considered in the error bars.

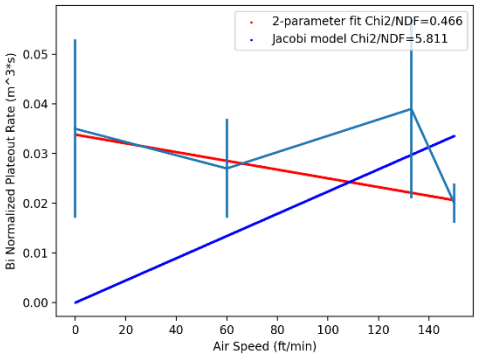

Figure 14: Acrylic Bi normalized plate-out rate vs air speed

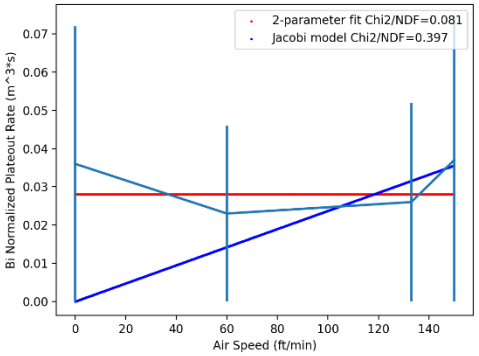

Figure 15: Acrylic Pb normalized plate-out rate vs air speed

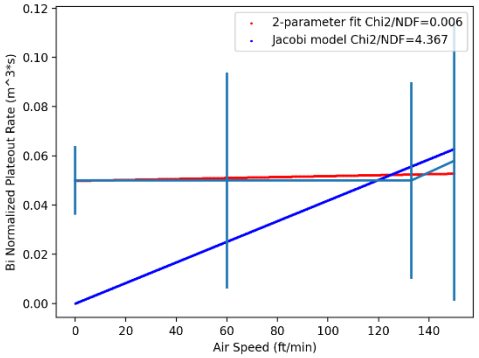

Figure 16: Acrylic Pb+Bi normalized plate-out rate vs air speed

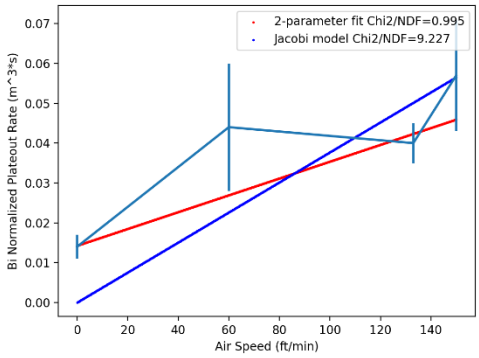

Figure 17: Copper Bi normalized plate-out rate vs air speed

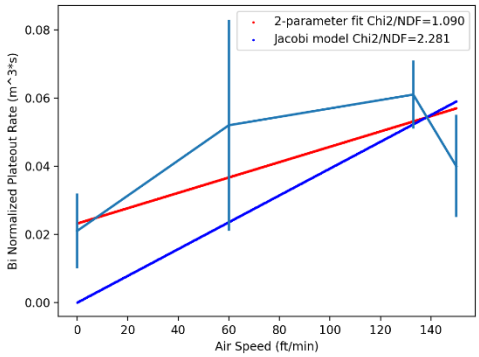

Figure 18: Copper Pb normalized plate-out rate vs air speed

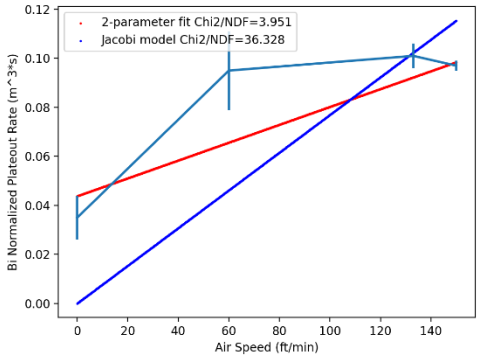

Figure 19: Copper Pb+Bi normalized plate-out rate vs air speed

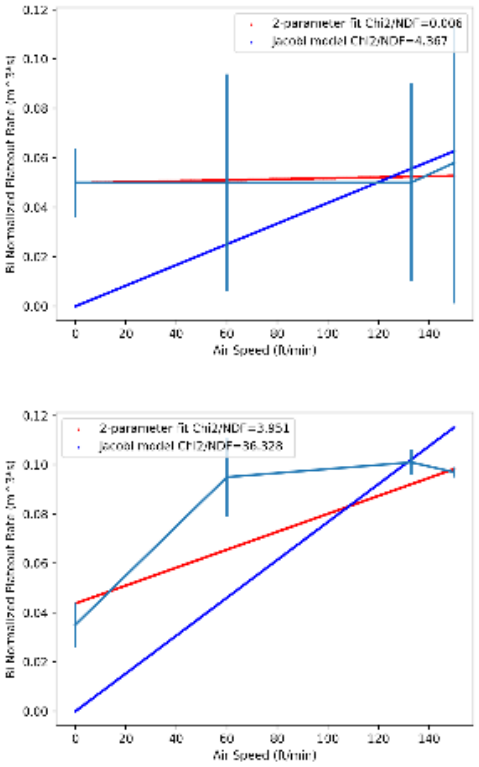

Figure 20: Acrylic and Copper Pb+Bi normalized plate-out rate vs air speed

Figure 20 compares the acrylic and copper results for normalized radon progeny plate-out rates, for both ^{214}Pb and ^{214}Bi. In comparing the plate-out trends, there are key differences between acrylic and copper, with acrylic offering interesting results. The trendlines are second-degree polynomial functions. The reduced χ^2 values, calculated as χ^2/NDF, indicate how closely the points align with the function, with a value of 1 demonstrating an ideal fit.

The acrylic samples demonstrate a relatively little correlation between plate-out and air speed. It is clear that the acrylic graphs do not display exponential trends, nor do they conform to a pattern of increasing or decreasing concentrations. Rather, with the fluctuations of ^{214}Pb and ^{214}Bi, the sum of both radon progeny results in a flat graph with little growth as fan speed increases. The impact of air speed on radon progeny plate-out for acrylic samples draws a contrast to the Jacobi model, which predicts a positive correlation between deposition velocity and plate-out rate. These results are therefore inconsistent with predictions and require further investigation to determine the reason for a neutral plate-out correlation.

Copper plate-out has a better agreement with the Jacobi prediction between plate-out and fan speed, with an χ^2/NDF value of 3.951. However, the greatest increase in radon concentration takes place between 0 to 60 ft/min air speeds, while faster speeds up to 150 ft/min do not generate significant additional plate-out. Therefore, while the Jacobi model is more in agreement with the copper results, it is still inconsistent with the plateau of radon progeny plate-out beyond air speeds of 60 ft/min.

A. Recommendations

According to the plate-out trends of acrylic and copper with respect to air speed, several recommendations are proposed. For acrylic, the lack of correlation between air speed and plate-out is important for considering the flow rate in the purge cabinets. When dark matter detectors or other equipment are stored in polycarbonate purge cabinets, N2 gas is blown through the cabinet to remove radon accumulation in the air. Given our results, the flow rate of N2 gas can be increased in purge cabinets to remove radon at a faster rate, with less concern about affecting how radon might plate-out on polycarbonate samples or on the cabinet surface itself. This also means antistatic fans could be operated inside purge cabinets to remove charge build-up without affecting plate-out rates.

The copper results indicate that the ideal environmental factors for minimizing radon progeny plate-out would occur at an air flow of 0 ft/min, or as low as possible. This could be considered in the surroundings of the dark matter detectors by setting up wind shields or taking additional measures to reduce air speed in the experimental surroundings. However, since plate-out also plateaus for air speeds greater than 60 ft/min, in conditions with unavoidable wind speed, greater air speeds would not significantly affect plate-out rates, as there is no linear correlation.

6. CONCLUSION

In this experiment, the antistatic fan and field source successfully reduced the inconsistency of electric charge in polycarbonate. This demonstrates an effective solution to the initial inconsistencies in plate-out measurements caused by electric charge build-up. It is important to note the greater range of uncertainty for the acrylic runs, which may relate to the variable nature of the material and how that might affect the plate-out [11].

These results disagree with the Jacobi model, as the acrylic results do not follow the linear relation of velocity and deposition rate. For the polycarbonate samples, potential causes for the deviations from the linear predictions of the Jacobi plate-out model could include the deposition of attached progeny and surface saturation. The deposition of attached progeny relates to the attachment of radon to dust particles in the air during circulation, which could alter the behavior of plate-out. Surface saturation would relate to the texture of acrylic, which by nature is more porous than the polished copper samples [14]. These porous or textured surfaces may be reaching progeny saturation, at which point air flow no longer affects the deposition rate. Future studies could continue to measure the electric charge of samples and determine if the field source could be a viable solution for charged surfaces in other areas of the experiment.

The Jacobi method is a significant approximation relying on key assumptions that a wind tunnel operates like a room at decay equilibrium from the Pylon Rn source. Future studies could gather more data to establish or refute the results of this study, particularly in comparing acrylic and copper. The Jacobi model also does not adequately capture the plate-out trends for copper, which demonstrate an increase in plate-out corresponding to air speed but appears to level out at velocities somewhere between 0 - 60 ft/min. This could indicate that different materials require different environments to minimize radon progeny plate-out, and is a viable next step for future experiments to investigate. Developing a more accurate model of radon progeny plate-out rate in varying environmental factors would enable researchers to implement stronger background mitigation measures against radon progeny plate-out in future experiments, like SuperCDMS.

A. Next Steps

This experiment provided a preliminary understanding of radon progeny plate-out on copper and polycarbonate at 4 SCFH of radon-spiked N2 gas for air speeds between 0 - 150 ft/min. Future studies can explore a broader range of air speeds to capture more comprehensive data. This could also be expanded by adjusting the rate of N2 gas input, testing similar air flow conditions in a purge cabinet, or building an experimental setup more similar to the storage rooms for dark matter detectors.

While the electric charge issue was addressed through the field source, the experiment could have further studies conducted for confirmation. Limitations also involved the Durridge RAD7, as a lack of measurement data for several trials required interpolation for the equilibrium values by taking the average of the existing Rad7 equilibrium data values. By refining the electric charge measurements and conducting more trials, the error margin of the plate-out results, particularly for acrylic, could be improved. Another approach to the electric charge issues would be to build a conductive wind tunnel or coat the interiors with a conductor. This would reduce the suspected triboelectric effect of air flow generating friction and creating charge on the polycarbonate walls. This could be more effective in blocking other contaminants.

8. ACKNOWLEDGEMENTS

I would first like to thank Dr. Jodi Cooley and Taylor Wallace for their guidance and mentorship throughout this research project, and for building a strong foundation for future work in radon plate-out. In addition, I would also like to thank Dr. Robert Calkins for his advice, patience, and support. Through numerous experimental runs, coding issues, and revisions, his advice has been invaluable in the development of this work. Dr. Calkins also showed me what it truly looks like to pursue curiosity and learning as the foundation of scientific research; this thesis would not have been possible without his contributions. Lastly, I want to thank my parents and brother for their encouragement throughout the highs and lows of my undergraduate career, and for walking alongside me to the finish line.

This work is supported by the National Science Foundation, the SMU Hamilton Scholars Program, and the SMU Physics Department.

9. APPENDIX

Table 1: Mean Life / Equilibrium vs % Change in Electric Potential

% Change in Electric Potential	^{214}Bi Normalized Plate-out Rate (m^3*s)	^{214}Pb Normalized Plate-out Rate (m^3*s)	^{214}Pb + ^{214}Bi Normalized Plate-out Rate (m^3*s)
-72	0.039	0.041	0.081
0	0.034	0.021	0.055
35	0.043	0.004	0.047
70	0.051	0.032	0.083
73	0.023	0.038	0.061
80	0.031	0.014	0.045
82	0.041	0.025	0.066
95	0.021	0.035	0.056
99	0.05	0.006	0.056
101	0.031	0.02	0.051
104	0.019	0.035	0.054
104	0.01	0.049	0.058
136	0.044	0.014	0.058
142	0.096	0.075	0.171

10. REFERENCES

[1] Jacobi, W. "Activity and Potential Alpha-energy of 222Radon and 220Radon-daughters in Different Air Atmospheres." Health Physics 22(5):p 441-450, May 1972. https://journals.lww.com/health-physics/Abstract/1972/05000/Activity_and_Potential_Alpha_energy_of_222Radon.2.aspx

[2] Albakry, M.F., et al. "A Strategy for Low-Mass Dark Matter Searches with Cryogenic Detectors in the SuperCDMS SNOLAB Facility" SuperCDMS Collaboration, 16 Mar. 2022, e-Print: 2203.08463 [physics.ins-det]

[3] "Radioactive Decay." EPA, Environmental Protection Agency, 28 Apr. 2023, https://www.epa.gov/radiation/radioactive-decay.

[4] Smith, N.J.T. The SNOLAB deep underground facility. Eur. Phys. J. Plus 127, 108 (2012). https://doi.org/10.1140/epjp/i2012-12108-9

[5] A. Bradley, D.S. Akerib, H.M. Araújo, et al. "Radon-related Backgrounds in the LUX Dark Matter Search." Physics Procedia, Volume 61, 2015, Pages 658-665, ISSN 1875-3892, https://doi.org/10.1016/j.phpro.2014.12.067.

[6] "Equations of Radioactive Decay and Growth." (2001). https://canteach.candu.org/Content%20Library/20052806.pdf

[7] Morrison, Eric S., et al. "Radon daughter plate-out onto Teflon." AIP Conference Proceedings. Vol. 1921. No. 1. AIP Publishing LLC, 2018.

[8] J. Street, R. Bunker, E. H. Miller, R. W. Schnee, S. Snyder, J. So. "Radon mitigation for the SuperCDMS SNOLAB dark matter experiment." AIP Conf. Proc. 3 January 2018; 1921 (1): 050002. https://doi.org/10.1063/1.5018995

[9] Jonassen, Niels, and Bent Jensen. "Removal of Radon Daughters by Filtration and Electrostatic Plateout." Technical University of Denmark, Laboratory of Applied Physics, 1988.

[10] Raymond Bunker, Tsuguo Aramaki, Isaac J. Arnquist, Robert Calkins, Jodi Cooley, et al. "Evaluation and mitigation of trace Pb-210 contamination on copper surfaces." e-Print: 2003.06357 [physics.ins-det], 13 Mar 2020.

[11] Bruenner, S., Cichon, D., Eurin, G. et al. "Radon daughter removal from PTFE surfaces and its application in liquid xenon detectors." Eur. Phys. J. C 81, 343 (2021). https://doi.org/10.1140/epjc/s10052-021-09047-2

[12] "Top Quality Antistatic Desktop High Frequency Mini Ionizing Air Blower KF-06WR." Suzhou KESD Technology Co.,Ltd., https://www.kesd-ions.com/product/kf-06w-top-quality-antistatic-desktop-high-frequency-mini-ionizing-air-blower.html.

[13] "Milty Zerostat 3 Antistatic Gun." CMY, https://www.cmy.com.my/shop-online/milty-zerostat-3-anti-static-gun/.

[14] D. Cangialosi, H. Schut, M. Wübbenhorst, J. van Turnhout, A. van Veen. "Accumulation of charges in polycarbonate due to positron irradiation" Radiation Physics and Chemistry, Volume 68, Issues 3–4, 2003, Pages 507-510, ISSN 0969-806X, https://doi.org/10.1016/S0969-806X(03)00219-6.

[15] Wallace, Taylor. "Evaluating the Impact of Airflow on Radon Plate-out Rates." Southern Methodist University, 2021.

[16] "Radioactive Sources: Pylon Electronics-Radon." Pylon Electronics - Instrument Manufacturing Division, 17 Mar. 2020, https://pylonelectronics-radon.com/radioactive-sources/.